Marine Chemistry 220 (2020) 103764

Contents lists available at ScienceDirect

Marine Chemistry

journal homepage: www.elsevier.com/locate/marchem

Characterization of the nonlinear salinity dependence of glass pH electrodes: A simplified spectrophotometric calibration procedure for potentiometric seawater pH measurements at 25 °C in marine and brackish waters: $0.5 \leq S \leq 36$

Loraine Martell-Bonet, Robert H. Byrne*

College of Marine Science, University of South Florida, 140 Seventh Avenue South, Saint Petersburg, FL 33701, United States

ARTICLE INFO

Keywords:
Electrode
Spectrophotometric calibration
Potentiometric measurements
Seawater pH

ABSTRACT

Glass electrodes are commonly used to measure the pH of natural waters over various, sometimes wide, ranges of salinity (S). For such applications, the electrodes must be calibrated against solutions of known pH and salinity identical to those of the sample solutions. Well-characterized buffer solutions may be used for these calibrations, but if a wide range of salinity is to be encountered in the samples (e.g., as in estuarine transects), this approach is quite laborious. Previous work has demonstrated that for $28.5 < S < 36.1$, pH electrodes can be efficiently calibrated spectrophotometrically in seawater because electrode intercept potential E_0 (a key calibration parameter) varies linearly with salinity over that range. The present work (a) characterizes pH electrode calibration parameters in seawater over a wider range of salinity ($0.5 < S < 36$) and (b) provides a simple and efficient method for creating and maintaining "river-to-sea" electrode calibrations over periods of months. Electrode calibration slope (g) was found to be insensitive to salinity, as expected. The value of this parameter, measured at $S > 5$, was reliably consistent with theoretical expectations, such that repeat verification needs to be conducted only occasionally. Electrode intercept potential (E_0), in contrast, was found to depend substantially on salinity: approximately linearly for $5 \leq S \leq 36$ and substantially nonlinearly for $0.5 \leq S < 5$. Ignoring this dependence of E_0 on S can lead to pH misestimates as large as 0.24, with the problem being most severe at lower salinities. Based on these observations, a method was developed by which the dependence of E_0 on S can be rapidly ascertained by simultaneously measuring pH (spectrophotometrically) and electromotive force (potentiometrically) in seawater that is serially diluted to produce the full range of salinities to be encountered in sampling. Because no acid titrations are required, a full river-to-sea calibration can be acquired in <3 h. With occasional (daily to weekly) one-point checks/corrections for electrode drift, this calibration is stable for weeks to months.

1. Introduction

Glass electrodes are widely used to measure solution pH due to their low cost, structural simplicity, and ease of use. Potentiometric (i.e., electrode) pH measurements can be expressed in terms of the electromotive force (emf) developed by a glass electrode–reference electrode pair (Buck et al., 2002):

$$\mathrm{pH}(X) = \mathrm{pH}(S_B) - (E_x - E_B)/(R_G T \ln 10/F) \quad (1)$$

where pH(X) is the pH of the sample solution, pH(S_B) is the pH of a standardizing solution (typically a carefully prepared buffer), E_x is the measured emf developed in the sample, and E_B is the measured emf developed in the buffer solution. The term $R_G T \ln 10/F$ is composed of the gas and Faraday constants (R_G and F) and the measured Kelvin temperature (T). At a temperature of 298.15 K, the magnitude of $R_G T \ln 10/F$, hereafter designated as g, is 59.16 mV.

Eq. (1) implicitly shows that the quality of potentiometric pH measurements is strongly dependent on the appropriate use of standardizing solutions. To ensure the accuracy of such measurements in seawater, it is essential that (a) the compositions of the buffer solutions used for electrode calibration closely match the compositions of the seawater samples to be analyzed (Whitfield et al., 1985; Millero, 1986; Dickson et al., 2007) and (b) the pH(S_B) values of the buffer solutions are well known (e.g., not compromised during long-term storage)

* Corresponding author.
E-mail address: rhbyrne@usf.edu (R.H. Byrne).

https://doi.org/10.1016/j.marchem.2020.103764
Received 16 July 2019; Received in revised form 21 January 2020; Accepted 25 January 2020
Available online 28 January 2020
0304-4203/

(Byrne, 1987; Nemzer and Dickson, 2005). Because of the importance of matching the composition of the buffer solutions to the composition of the seawater samples (Riebesell et al., 2011), careful preparation of multicomponent seawater buffers (Millero et al., 1993) has been regarded as essential to obtaining accurate potentiometric seawater pH measurements.

As a convenient alternative to preparing a series of seawater buffers, Easley and Byrne (2012) demonstrated the efficacy of calibrating electrodes directly in seawater with the use of the spectrophotometric pH indicator meta-cresol purple (mCP). The principle of the method is described by:

$$\mathrm{pH}(X) = (E_0 - E_X)/g' \tag{2a}$$

$$E_X = -\mathrm{pH}(X)\bullet g' + E_0 \tag{2b}$$

where pH(X) is the spectrophotometrically measured pH of the seawater sample, E_x is the emf developed by the potentiometric pH cell, E_0 is the electrode intercept potential (i.e., E_x extrapolated to pH(X) = 0), and g' is the experimentally determined electrode slope (i.e., the slope of a line that describes measured potentiometric E_x as a function of measured spectrophotometric pH(X)). With conjugate measurements of spectrophotometric pH(X) and potentiometric E_x (absolute millivolt mode) made in the calibrating seawater, linear regression of E_x against spectrophotometric pH(X) yields g' (the slope of the regression line) and E_0 (the intercept of the line). For an electrode behaving ideally at a Celsius temperature (t) of 25 °C, the slope would be 59.16 mV (the so-called Nernstian slope). Spectrophotometric pH is defined on the total hydrogen ion scale ($\mathrm{pH_T}$).

If the salinity (S) dependence of E_0 is well characterized over a range of salinity, then the pH of seawater samples within that same range can be determined from measurements of E_x in the samples. Easley and Byrne (2012) characterized the salinity dependence of E_0 for Orion Ross pH electrodes (model 8102BN) over the range of $28.5 \le S \le 36.1$ (at t = 25 °C). This limited S range was constrained by the mCP characterization that was available at the time (i.e., the salinity range within which the relevant characteristics of the indicator were well defined).

Recently, several "river-to-sea" characterizations of mCP ($0 \le S \le 40$) have been developed (e.g., Douglas and Byrne, 2017; Müller and Rehder, 2018), thus providing an opportunity to extend the electrode calibration method of Easley and Byrne (2012) to a much wider range of natural and laboratory waters. In this work, electrode behavior is characterized over the salinity range of $0.50 \le S \le 36$ (t = 25 °C) and a method is developed to rapidly calibrate glass pH electrodes for measurements over that range. The overarching objective is to provide a simple protocol for obtaining accurate potentiometric pH measurements, free of calibration bias, over a river-to-sea continuum of salinities.

2. Theory of spectrophotometric electrode calibration

The core of the method described here is the simultaneous measurement of E_x (using a high-quality glass pH electrode) and $\mathrm{pH_T}$ (using a high-quality spectrophotometer and the indicator mCP) in a series of seawater-based calibrating solutions that encompass an experimentally relevant and application-specific range of salinities.

2.1. Spectrophotometric pH measurements

Meta-cresol purple is widely used for spectrophotometric measurements of oceanic seawater pH over a range of 7.2 to 8.2. Sulfonephthalein indicator dyes such as mCP are used to measure hydrogen ion concentration ($[H^+]$) in solution, based on measured absorbance ratios of the protonated (HI^-) and unprotonated (I^{2-}) indicator species in the sample solution (Clayton and Byrne, 1993). The works of Douglas and Byrne (2017) and Müller and Rehder (2018) provide comprehensive algorithms for using mCP to measure $\mathrm{pH_T}$ in fresh water, estuarine water, and seawater over wide ranges of salinity ($0 \le S \le 40$) and temperature ($278.15 \le T \le 308.15$ K). For all such models, pH on the total hydrogen ion concentration scale is parameterized using:

$$\mathrm{pH_T} = \log(K_2 e_2) + \log\left(\frac{R - e_1}{1 - R\frac{e_3}{e_2}}\right) \tag{3}$$

The parameter K_2 is the dissociation constant of HI^- on the total hydrogen concentration scale: $K_2 = [I^{2-}][H^+]_T[HI^-]^{-1}$. The parameter R is the ratio of mCP absorbances (A) measured in the sample at 578 nm and 434 nm: $R = {}_{578}A/{}_{434}A$. The quantities e_1, e_2, and e_3 are the ratios of the molar absorption coefficients (ε) of the HI^- and I^{2-} indicator forms (i.e., expressions of light attenuation per mole for the pure HI^- and I^{2-} species at specified wavelengths). For mCP, these terms are defined as $e_1 = {}_{578}\varepsilon_{HI^-}/{}_{434}\varepsilon_{HI^-}$, $e_2 = {}_{578}\varepsilon_{I^{2-}}/{}_{434}\varepsilon_{HI^-}$, and $e_3 = {}_{434}\varepsilon_{I^{2-}}/{}_{434}\varepsilon_{HI^-}$. The $\log(K_2 e_2)$ term can be expressed as a single product of molar absorption and dissociation constant parameters ($K_2 e_2$) at 25 °C (Zhang and Byrne, 1996). For this work, parameterizations of all terms in Eq. (3) were taken from the work of Müller and Rehder (2018).

2.2. Characterization of salinity-dependent electrode behavior

Eq. (2a) shows that the two elements of the spectrophotometric electrode calibrations are assessments of electrode slope, g', and determinations of electrode intercept, E_0. The measurements of g' are used to assess whether an electrode is working properly. This term should be examined on a regular basis, and electrodes that consistently exhibit deviations of more than 0.3% from ideal Nernst behavior should be replaced (DOE, 1994). The magnitude of g' is temperature dependent, but no dependence on salinity has been documented. As noted in Section 1, the theoretical Nernst slope at a temperature of 298.15 K is 59.16 mV. For other temperatures, the theoretical slope can be calculated by:

$$g(T) = 59.16\ \mathrm{mV}\bullet\left(\frac{T}{298.15\ \mathrm{K}}\right) \tag{4}$$

The magnitude of the E_0 term depends on a number of factors, including electrode design/construction, the composition of the electrode filling solution, and the temperature, composition, and concentration of the sample solution. E_0 can be calculated in two ways: (a) from linear regressions of E_x versus pH(X) (Eq. (2b)) or (b) from an assumption of $g' = g$ and then solution of Eq. (2b) for E_0 at a single spectrophotometrically determined $\mathrm{pH_T}$. When the samples of interest encompass a range of salinities (e.g., as in a typical estuarine transect), an electrode-dependent function describing the dependence of E_0 on S must be defined (i.e., parameterized). In this work, plots of E_0 versus S were fitted to the following function by least squares analysis using MATLAB:

$$E_0 = A + \frac{B\,S^{1/2}}{1 + C\,S^{1/2}} + D\,S \tag{5}$$

where A, B, C, and D are fitting parameters.

3. Materials and methods

3.1. Materials

Unpurified mCP powder was obtained from Acros Organics (lot AC199250050) and subsequently purified using the procedures of Liu et al. (2011); stock solution was formulated with a concentration of 10 mM. Open-ocean seawater was collected from the Gulf of Mexico ($S \approx 36$). The salinities of all seawater samples (original and diluted) were measured with a YSI Professional Plus sensor (PRO 30 COND-T

16A100370; salinity resolution of ±0.1) that was calibrated with a Portasal Salinometer (model 8140A). Solutions of NaOH (catalog number SS266-1, lot 127455) and HCl (catalog number SA48-1, lot 127672) were obtained from Fisher Scientific. Bicarbonate titrants were formulated from $NaHCO_3$ solution (BioXtra, 99.5–100.5%) obtained from Sigma-Aldrich (catalog number S-6297, lot 50 K0241). NaCl was obtained from MP Biomedicals (catalog number 102892, lot M1620).

Spectrophotometric pH measurements were made using an 8453 HP spectrophotometer. Potentiometric measurements were obtained using two Orion Ross glass pH electrodes (model 8102BNUWP) and an Orion pH meter (model 720A; 0.1 mV resolution) in the absolute millivolt mode. Both sets of measurements were obtained in a custom-made, open-top spectrophotometric quartz cell (10 cm path length, 150 mL volume) housed in a thermostatted (25.00 ± 0.05 °C) custom-made spectrophotometer cell compartment connected to a Lauda Ecoline RE120 water bath. Sample temperatures were recorded using a Fisher Scientific Traceable digital thermometer (catalog number 15-077-8). A Gilmont micrometer dispenser burette (GS-1200) was used to deliver small increments of titrant. During the time between experiments, the electrodes were stored in 0.1 M HCl.

3.2. Electrode slope and potential as a function of salinity (seawater): titration-based method

The behaviors of the glass electrodes in seawater were characterized over ranges of salinities and pH. Ranges of salinity were obtained by diluting seawater with deionized water to produce a solution series of $0.5 \le S \le 36$, with increments of approximately $\Delta S = 1$. At each new salinity, a range of pH was obtained by manually titrating the seawater with 0.1 M HCl to achieve pH_T values over the range of 6.7 to 8.6 (corresponding to an R range of 0.04 to 2.5). At each titration point, simultaneous measurements were made of spectrophotometric pH(X) and electrometric E_x (7 to 19 data pairs per salinity). Finally, least squares linear analysis of these data (Eq. (2b)) was used to yield estimates of g' and E_0 at each salinity.

Each titration began with measurement of a reference blank (i.e., background absorbance of the seawater sample). Stock mCP solution was then added to obtain an mCP concentration of approximately 2.0×10^{-6} M, and absorbances were measured at the mCP absorbance peaks of 434 nm and 578 nm and at the non-absorbing (baseline-correction) wavelength of 730 nm (Clayton and Byrne, 1993; Liu et al., 2011). Throughout each titration, the seawater was mixed with an overhead stirrer; absorbance measurements indicated that complete mixing required approximately 90 s. After the rate of change of electrode potential became stable (i.e., drift ≤0.10 mV over two minutes), spectrophotometric R and electrometric E_x were recorded. Seawater pH_T was then calculated from R, using Eq. (3) as described by Müller and Rehder (2018). Our analyses were confined to observations where $0.1 \le R \le 2$ (i.e., well within the operational range of mCP). For seawater samples with $S \le 5$, it was necessary to add NaOH to achieve initial R values between 1.5 and 2. These experiments were conducted using electrode filling solutions of 0.7 M and 3 M NaCl.

3.3. Electrode potential as a function of ionic strength (NaCl)

As an assessment of E_0 behavior independent of the spectrophotometric pH_T observations (i.e., to assess whether E_0 observations might include artifacts related to the spectrophotometric measurements), electrode potentials were also observed in simple NaCl solutions at pH = 2.70 (H^+ concentration = 2×10^{-3} M) over a range of ionic strengths: $0 \le I \le 0.70$. This range of I was achieved by mixing acidified deionized water (0.002 M HCl) with 0.7 M NaCl solutions that contained 0.002 M HCl. In these experiments, then, the pH (on the free hydrogen ion concentration scale) was known rather than measured: $pH = -\log(2 \times 10^{-3}) = 2.699$.

Two types of measurements were performed: measurements with solutions of 0.698 M NaCl plus 0.002 M HCl, and measurements with solutions of 0.098 M NaCl plus 0.002 M HCl (whereby all solutions contained 2×10^{-3} M HCl). The solutions were mixed with an overhead stirrer. These experiments were conducted using electrode filling solutions of 0.7 M and 3 M NaCl. Electrode potentials (absolute mV) as a function of ionic strength were recorded at 25 °C. Eq. (2b) was then used with the known pH to calculate E_0. The results of these experiments are reported as E_0 versus I.

3.4. Electrode potential as a function of salinity (seawater): Rapid, no-titration method

Simple, titration-free electrode calibrations provide an efficient alternative to the laborious electrode calibrations described in Section 3.2. With this approach, Nernstian electrode behavior, once demonstrated, is thereafter assumed. Therefore, the HCl titrations described in section 3.2 can be eliminated and only a single pair of E_x–pH_T measurements is required at each salinity. For this work, values of E_x and pH_T were simultaneously recorded as seawater was successively diluted over the range $0.35 \le S \le 36.20$.

This series of observations was begun by measuring background sample absorbances in full-strength seawater. A solution of purified mCP was then added to yield an mCP concentration of approximately 2.9×10^{-6} M. Absorbances of mCP were measured at the usual three wavelengths, and E_x was recorded. The sample was then diluted by addition of 2 mM $NaHCO_3$ solution, to produce a sample of lower salinity but roughly comparable buffer intensity. Absorbance measurements indicated that complete mixing of the cell contents required 120 to 240 s. Because these additions increased the volume of solution in the open-top cell, a pipette was used to remove fully mixed solution, as needed, to prevent overflow. Additional mCP was added, as needed, to maintain a roughly constant indicator concentration. Eq. (2b) was then used with each pair of E_x and pH_T observations to generate values of E_0 as a function of S. Finally, MATLAB was used to quantitatively describe (parameterize) E_0 as a function of S, according to the function given in Eq. (5).

4. Results and discussion

4.1. Characterization of electrode behavior in seawater: g' and E_0

The result of a typical spectrophotometric electrode calibration, whereby electrode potential is plotted against spectrophotometric pH_T (Eq. (2b)), is shown in Fig. 1. This electrode exhibited ideal Nernstian

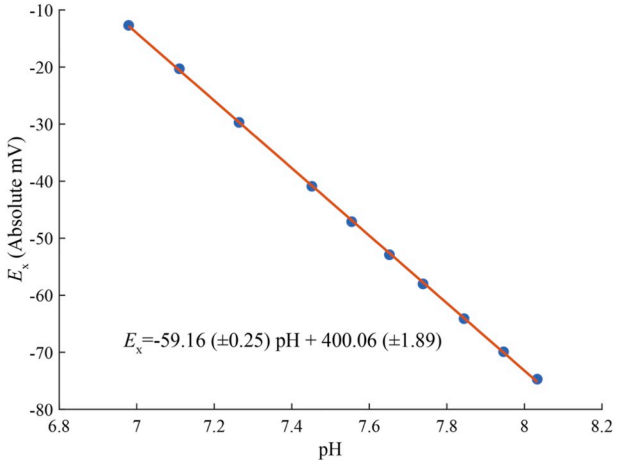

Fig. 1. Results from a typical spectrophotometric electrode calibration in a sample of natural seawater (S = 19.50, t = 24.92 ± 0.05 °C, r^2 = 0.9999; electrode 1).

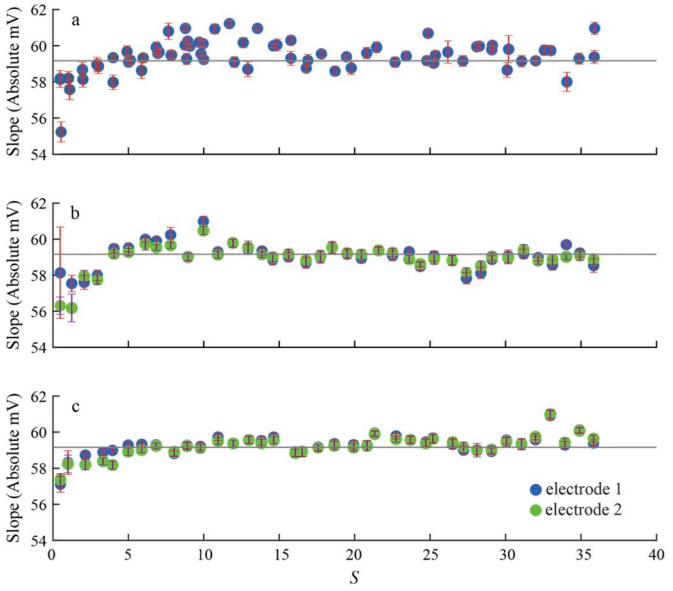

Fig. 2. Electrode calibration slopes experimentally determined over $0.49 \leq S \leq 35.91$. Each panel represents a different series of seawater dilutions. Each dot represents electrode slope as determined by acid titration at each salinity. The depicted uncertainties represent standard errors (1σ). The horizontal gray lines show the theoretical Nernst slope of 59.16 mV at $t = 25$ °C. These data are summarized in Table 1, and the full data sets are given in Appendix A. Panel (a) shows data obtained over a period of 44 days using a single electrode with a 0.7 M NaCl filling solution. Panel (b) shows data obtained using two electrodes with 0.7 M NaCl filling solutions over a period of 9 days. Panel (c) shows data obtained over a period of 14 days using two electrodes with 3 M NaCl filling solutions.

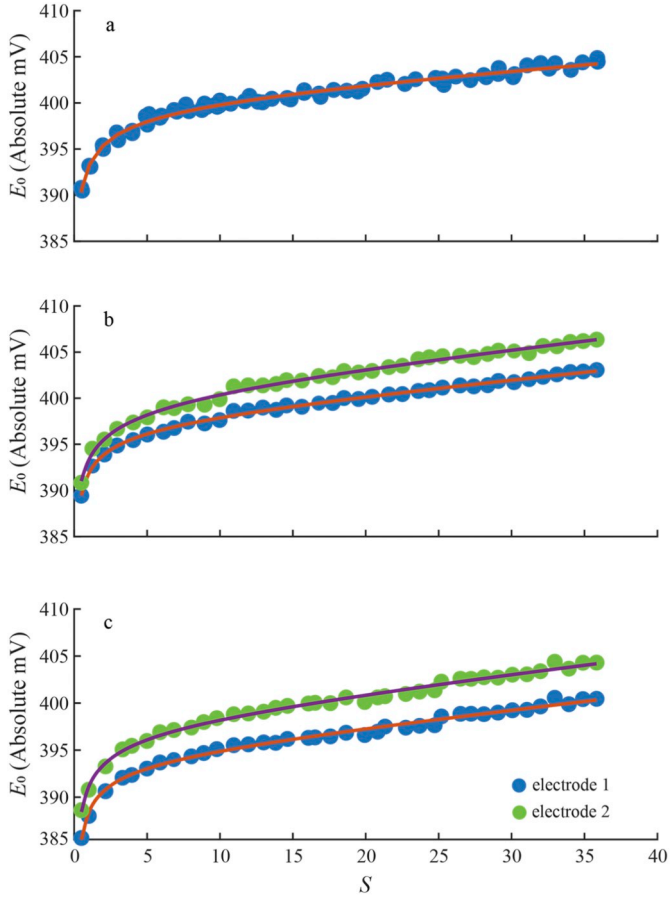

Fig. 3. E_0 as a function of salinity, obtained using multiple paired measurements of E_x and pH_T at each salinity (the same data used to generate corresponding Fig. 2a, b and c) and an assumed ideal (Nernst) electrode slope (i.e., $g' = g$) at every salinity. Each dot represents the average of all E_0 values obtained at the given salinity. The solid lines represent the nonlinear least squares fit lines obtained with Eq. (5). The best-fit coefficients (A, B, C, D) used to generate these curves are given in Appendix B.

behavior: the measured slope g' was 59.16 ± 0.25 mV, which is very close to the theoretical Nerstian slope of 59.14 mV at the experimental temperature of 24.92 °C (Eq. (4)). The value of E_0 (the y-intercept) calculated from the Fig. 1 linear fitting equation is 400.06 ± 1.89 mV.

4.2. Electrode calibration slope as a function of salinity

Calibration slopes obtained for the two glass electrodes over the salinity range of $0.49 \leq S \leq 35.91$ are shown in Fig. 2. The slopes and intercepts obtained for each fit are given in tabular form in Appendix A. Each data point in Fig. 2 represents the slope obtained from fitting a multipoint calibration (titration) data set at the given salinity (i.e., measurements of E_x versus pH, as shown in Fig. 1, at each salinity). Between salinities of 36 and 5, the electrodes closely conformed to the expected Nernstian behavior, with slopes of approximately 59.16. At lower salinities, the observed slopes systematically fell to significantly lower values. The slope data for the three sets of calibrations are summarized in Table 1. These results, obtained over a period of nearly 5 months (see Appendix A), indicate that electrode slope behavior is stable on a timescale of months.

The observations shown in Fig. 2a and b were obtained with a 0.7 M NaCl filling solution, and the Fig. 2c results were obtained with a 3 M NaCl filling solution. Comparison of the average calibration slopes for these data sets (Table 1) shows that electrode slopes were not markedly influenced by the concentration of the filling solution.

Because a salinity influence on electrode slope is not expected on the basis of any theoretical considerations or prior observations, we interpret the systematic decreases in g' at $S < 5$ as likely artifacts, due to factors other than a direct response of the glass electrode membrane to hydrogen ion concentrations or activities. One potential cause is the very strong influence of salinity on the mCP $\log(K_2 e_2)$ term (Eq. (3)) at low salinities (Douglas and Byrne, 2017; Müller and Rehder, 2018). Because of this sensitivity, small salinity changes in the course of a

Table 1
Electrode calibration slopes (mean ± standard error) obtained in seawater over ranges of salinity (least-squares, titration-based approach). The data are shown in Fig. 2.

Figure	Electrode	Filling solution (M NaCl)	Duration of experiment	Average g' for $S < 5$	Average g' for $5 \leq S \leq 36$
2a	1	0.7	44 days	58.25 (±0.36)	59.63 (±0.09)
2b	1	0.7	9 days	58.14 (±0.35)	59.18 (±0.10)
	2	0.7		57.48 (±0.56)	59.14 (±0.07)
2c	1	3.0	14 days	58.55 (±0.32)	59.43 (±0.07)
	2	3.0		58.22 (±0.20)	59.40 (±0.07)

Slopes (g') have units of mV.

titration at $S < 5$ could lead to small errors in the calculated values of pH_T (Eq. (3)). Thus, a principal recommendation resulting from this work is that assessments of pH electrode slope (g') be performed at salinities greater than 5.

4.3. Intercept potential as a function of salinity

Fig. 3 shows averaged E_0 (intercept) values at each salinity calculated using the E_x and pH pairs used to generate Fig. 2, along with the assumption of an ideal Nernst slope ($g' = g$) over the entire range of S. This assumption is supported by the substantially Nernstian behavior exhibited by both electrodes for $S > 5$ (Fig. 2, Table 1). The Fig. 3 results show that for $S \geq 5$, the dependence of E_0 on salinity is approximately linear. For $S < 5$, however, the dependence is substantially nonlinear. Within the linear and nonlinear regions, the overall ranges of E_0 are approximately equal, with the observed E_0 variation (range) being approximately 7 mV for $5 \leq S \leq 36$ and 7 mV for $0.5 \leq S \leq 5$.

This strong and overall nonlinear dependence of E_0 on S has important implications: (1) an electrode calibrated at a single salinity cannot be used to provide quantitative pH measurements in settings where salinity can be highly variable (e.g., estuaries) and (2) the magnitude of pH misestimates caused by ignoring the dependence of E_0 on S can be quite large. For electrodes calibrated with a single Tris seawater buffer at $S = 35$, pH measurements made at $S = 5$ could be in error by 0.12; near $S = 0$, the pH errors could be as large as 0.24.

The dependence of E_0 on S is quantitatively well described by parameterizations in the form of Eq. (5) (Fig. 3). The parameters A, B, C, and D for the five fits shown in Fig. 3 are given in Table B1 of the supporting information. Residuals for these parameterizations (i.e., differences between observed and calculated values of E_0) are small and randomly distributed (see Fig. C1 in the supporting information). Eq. (5) and the fitting parameters shown in Table B1 allow for the calculation of changes in E_0 that are caused by either deliberate or inadvertent variations in S. For analyses at $S > 28.5$ (e.g., Easley and Byrne, 2012), a salinity change of 0.1 will yield a change in E_0 on the order of 0.06 mV or less. This change is equivalent to a pH change of 0.001 or less. For analyses at $S \approx 4.0$, a 0.1 unit change in salinity creates a change in E_0 on the order of 0.6 mV and, thereby, a pH change on the order of 0.01 (i.e., 10 times the change seen at an open-ocean salinity). For analyses at very low salinities, the variations in E_0 with salinity and, accordingly, the variations in calculated pH are even larger. This comparison demonstrates that electrode calibrations consistent with a pH measurement accuracy of ± 0.001 at low salinity ($S \leq 5$) require salinity measurements with an accuracy on the order of 0.01 or better. This shows that, along with the strong influence of salinity on spectrophotometric pH measurements at low salinity as described in Section 4.2, salinity-induced variations in E_0 for $S < 5$ can also contribute to the appearance of non-Nernstian electrode slopes (g') seen in Table 1.

Fig. 3 also shows that while the shapes of the five E_0-versus-S curves are substantially similar, the magnitudes of the E_0 values are different. Even for a single electrode, the curve may shift up or down over time. For example, note the low electrode 1 values of $E_0(S = 0)$ in Fig. 3c relative to Fig. 3a and b. In other words, although the curves shown in Fig. 3a–c are similar in shape, the intercept term A in Eq. (5) ($A = E_0$ at $S = 0$) may slowly change over a period of weeks to months. This tendency of A to drift must be accounted for in calibration procedures (as discussed below in Section 4.5).

4.4. Intercept potential (E_0) as a function of NaCl ionic strength

To more closely examine the nonlinearities seen in E_0 at $S < 5$ (Fig. 3) (i.e., to rule out the possibility of artifacts associated with mCP characteristics), we also measured E_0 over a range of ionic strengths ($0 \leq I \leq 0.7$ M) in simple solutions of acidified NaCl (Fig. 4). The ionic strength of seawater at $S = 35$ is approximately 0.7 M; at $S = 5$, I is approximately 0.1 M. In this set of experiments, the pH was known rather than measured. Nernstian electrode behavior was assumed, based on the ideal behavior and stability previously exhibited by the electrodes being used (Fig. 2).

The dependence of E_0 on ionic strength (Fig. 4) closely resembles the dependence of E_0 on salinity (Fig. 3). The variation of E_0 with I is approximately linear for $0.1 \leq I \leq 0.7$ M but is substantially nonlinear for $I < 0.1$ M. The change in E_0 within the linear segment is approximately 10 mV, and the change in the nonlinear segment is approximately 14 mV. These results, which are relevant to pH observations on the free hydrogen ion concentration scale, show substantially larger E_0 variations than those obtained on the total hydrogen scale (Fig. 3).

The dependencies of E_0 on S and I (Figs. 3 and 4) are attributable to a number of factors. One important influence is the variation of liquid junction potentials (Kadis and Leito, 2010) created by variable

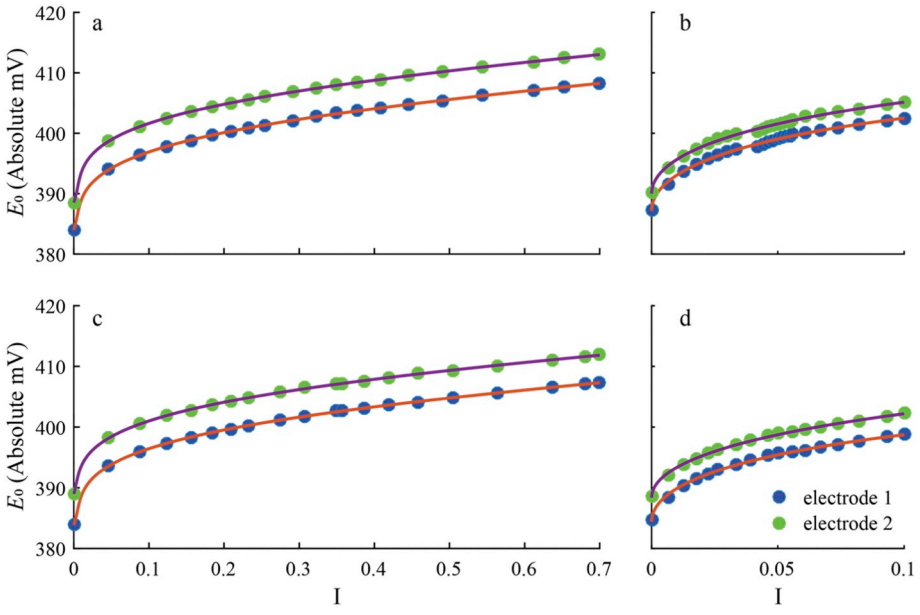

Fig. 4. E_0 as a function of ionic strength in acidified NaCl solutions. The results shown in panels (a) and (c) were performed over a range of ionic strength corresponding to dilutions of $S = 35$ seawater. Panels (b) and (d) show E_0 variations that correspond to dilutions of $S = 5$ seawater. Measurements in panels (a) and (b) were performed using 0.7 M NaCl electrode filling solution and panels (c) and (d) show observations using 3 M NaCl electrode filling solution. Solid lines represent nonlinear least squares fits obtained with Eq. (5).

concentration gradients between electrode filling solutions (constant composition) and external seawater or NaCl solutions (variable composition or concentrations). Other important determinants include variations in hydrogen ion activity coefficients with changing salinity and ionic strength (Millero and Schreiber, 1982) and, in the case of seawater, variations in the extent of HSO_4^- formation with changing salinity (DOE, 1994). However, it should be noted that while free H^+ activity coefficients at $S = 0$ ($\gamma(H^+) = 1$) and $S = 35$ ($\gamma(H^+) = 0.967$) are both greater than $\gamma(H^+)$ at $S = 5$ ($\gamma(H^+) = 0.824$) (Millero and Schreiber, 1982), E_0 shows a monotonic increase with increasing salinity over this range of conditions (no inflection is observed in the dependence of E_0 on S shown in Fig. 4). As such, it appears that the S and I dependence of H^+ activity coefficients is not the dominant factor controlling the behavior of E_0 over the full range of S and I conditions shown in Figs. 3 and 4. A plausible explanation for the E_0 behavior evident in those figures is a largely linear influence of S and I on liquid junction potentials over $0 \le S \le 35$ and $0 \le I \le 0.7$ M, in combination with the additional (nonlinear) influence of rapidly changing activity coefficients over $0 \le S \le 5$ and $0 \le I \le 0.1$ M.

4.5. Rapid, no-titration calibration procedure for potentiometric river-to-sea pH measurements

The complex, titration-based calibration method described in Section 3.2 (with results shown in Sections 4.1 through 4.3) is thorough but laborious. As a result, only two or so titration lines (e.g., Fig. 1) can be produced per day. Characterizing electrode behavior over the full river-to-sea range of salinities (e.g., Fig. 3a) therefore requires a minimum of one to two weeks. Consequently, this calibration method is not practical for routine applications. An alternative procedure was therefore developed, whereby complete characterization of E_0 over a wide range of S can be obtained in one to three hours.

With this simplified approach, natural or synthetic seawater is incrementally diluted with a 2 mM solution of $NaHCO_3$ (thus maintaining buffer intensity) to encompass the salinity range of interest (in this work, $0.5 \le S \le 36.1$). Temperature is held constant (in this work, nominally at 25 °C). At each new salinity, only a single E_x and pH_T pair is measured (no acid titration); temperature is also measured. With the assumption of $g' = g$ (with g calculated for the measured temperature; Eq. (4)), a salinity-specific value of E_0 can be calculated from Eq. (2b). Finally, Eq. (5) is used to fit the resulting plot of E_0 as a function of S.

Fig. 5 shows the results of this simplified approach. Consistent with the results of the full, titration-based calibrations (Fig. 3), the dependence of E_0 on salinity is seen to be approximately linear for $S \ge 5$ and nonlinear for $S < 5$. For the curves shown in Fig. 5a, 95% of the fitting residuals are <0.6 mV; for Fig. 5b, 100% of the residuals are <0.3 mV (see Fig. D1 in the supporting information).

Significantly, calibrations performed in this manner provide a means of obtaining quantitative pH_T data over a river-to-sea range of salinity yet require little more effort than that required to produce a single seawater buffer (which would be specific to only a single salinity). Acquisition of the calibration data shown in Fig. 5a and b took approximately 3 h and 1.5 h, respectively.

The electrode-specific dependence of E_0 on salinity (Fig. 5) should be characterized whenever potentiometric pH is to be measured in samples that encompass a range of salinities. Because E_0 is a time-dependent variable, measurements of E_0 must be made much more frequently than electrode slope assessments. Ideally, E_0 should be measured immediately before or after a series of measurements of samples. The S range of the calibration does not need to be as wide as the range shown here; it needs only to match the anticipated S range of the samples. The resulting fitting parameters are then used to calculate a salinity-specific value of E_0 (Eq. (5)) and pH_T (Eq. (2a)) appropriate for each sample.

A least-squares determination of electrode slope (e.g., Fig. 1) is still required every few weeks to verify that a given electrode continues to exhibit Nernstian behavior (i.e., to justify the assumption of $g' = g$, which is implicit in the $E_0(S)$ functions shown in Fig. 5). As indicated by the results shown in Fig. 2, this assessment of Nernstian response should be performed in a seawater sample of $S > 5$.

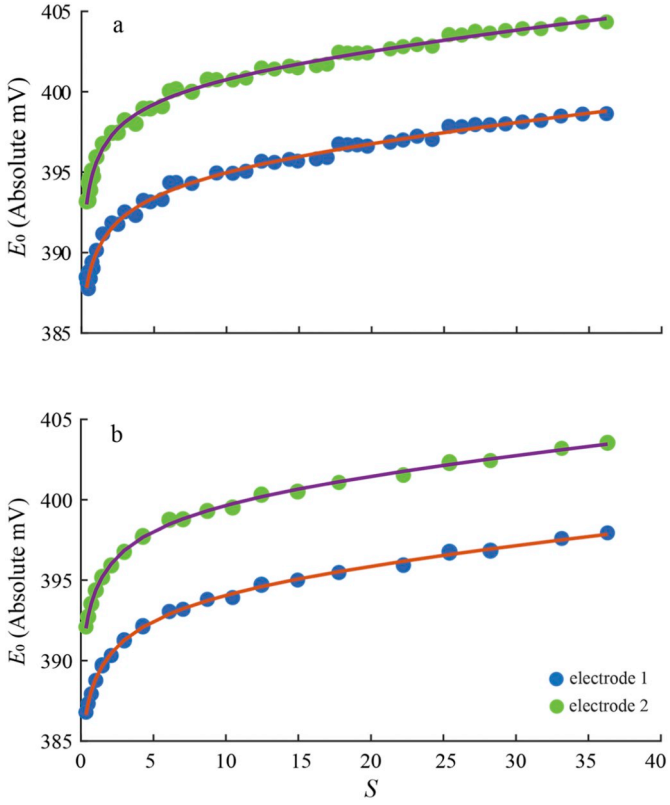

Fig. 5. E_0 as a function of salinity, obtained using the no-titration calibration procedure (i.e., a single measurement of E_x and pH_T at each salinity) and an assumed calibration slope of 59.16 mV. The electrode filling solution was 3 M NaCl. The results shown in panel (a) were obtained in ≈ 3 h and the panel (b) results were obtained in ≈ 1.5 h. Each dot represents the E_0 values obtained at the given salinity. The solid lines represent the nonlinear least squares fit lines obtained with Eq. (5). The best-fit coefficients (A, B, C, D) used to generate these curves are given in Appendix B.

If additional investigations with other electrodes confirm our observations that the parameter A in Eq. (5) tends to drift, then ideally this value should be updated immediately prior to measuring the pH of samples. This update can be achieved as follows: (a) measure E_x and spectrophotometric pH_T in a seawater sample of known salinity, (b) use Eq. (2b) and those measurements to calculate E_0, and (c) solve Eq. (5) for A, given this new value of E_0 and the previously determined values of B, C, and D.

5. Conclusions and implications

1. Our spectrophotometric electrode calibrations in seawater are consistent with the observations of Easley and Byrne (2012) in showing that salinity strongly influences potentiometric measurements of seawater pH. However, in contrast to the linear dependence of E_0 on salinity for the limited open-ocean salinity range of $28.5 < S < 36.1$, as observed by Easley and Byrne (2012), this work demonstrates that the dependence of E_0 on salinity over the wider salinity range of $0.5 \le S \le 36$ is nonlinear and that quantitative descriptions of those nonlinearities are needed. The procedures developed in this investigation provide a practical means for investigators to (a) rapidly characterize the dependence of E_0 on salinity for marine and brackish waters and (b) calculate E_0 as a smooth function of salinity over the entire salinity range, including

the transition from linear to highly nonlinear behavior.

2. The practice of calibrating a potentiometric electrode in a single buffer does not account for the influence of salinity on electrode behavior (specifically, E_0). Over a salinity range of 0 to 36, E_0 varies by ~14 mV (Fig. 3), which is equivalent to a pH variation or error of ~0.24. This potential problem can be obviated by characterizing E_0 as a function of S over the range of salinities to be sampled.
3. If an electrode is to be used to measure the pH of samples over a range of salinities, then that electrode must be calibrated in solutions spanning a similar range. This essential calibration can be accomplished with either (a) potentiometric measurements in a series of freshly prepared seawater buffers of known pH or (b) paired potentiometric and spectrophotometric measurements in serially diluted seawater. Formulating a series of complex buffers is more laborious than incrementally diluting natural seawater.
4. The dependence of E_0 on salinity curve appears to be substantially consistent over periods of weeks to months. For a given electrode, then, the B, C and D coefficients (Eq. (5)), which describe the shape of the E_0-versus-S curve (e.g., Fig. 5), can be considered as invariant over periods of weeks to months. However, the intercept term A (which is equal to E_0 at $S = 0$) is a less stable quantity. As a result, the E_0 vs. S curve, with its constant shape, may shift up or down over a period of days.
5. A simple protocol for maintaining calibrated electrodes could consist of the following steps:

(a) Confirm Nernstian electrode behavior at constant temperature and a single salinity of $S > 5$ (as described in Section 4.1 and shown in Fig. 1). We suggest that this confirmation (i.e., a single titration) be conducted every month or so.
(b) Determine the dependence of E_0 on salinity over an experimentally relevant range of S (as described in Section 4.5 and shown in Fig. 5). Parameterize these E_0-versus-S data with Eq. (5), thereby obtaining the coefficients A, B, C, and D. We suggest that this characterization be obtained approximately monthly.
(c) Update the less stable parameter A (as described in Section 4.5). We suggest that this update be performed approximately daily, immediately prior to the start of measuring the E_x and pH of seawater samples.

6. The simple spectrophotometric calibration method described in this paper allows for the calculation of salinity-dependent values of E_0 appropriate for potentiometric pH_T measurements of seawater samples with salinities within the range $0 \leq S \leq 36$.

Declaration of Competing Interest

None.

Acknowledgements

Funding for this project was provided by National Science Foundation award 1658321. Support for Loraine Martell-Bonet was also provided by the Bridge to the Doctorate Endowed Fellowship from the University of South Florida College of Marine Science. We thank Tonya Clayton for providing valuable editorial assistance. The authors gratefully acknowledge the comments of three anonymous reviewers.

Appendix A. Supplementary data

Supplementary data to this article can be found online at https://doi.org/10.1016/j.marchem.2020.103764.

References

Buck, R.P., Rondinini, S., Covington, A.K., Baucke, F.G.K., Brett, C.M., Camoes, M.F., et al., 2002. Measurement of pH. Definition, standards, and procedures (IUPAC recommendations 2002). Pure Appl. Chem. 74 (11), 2169–2200.
Byrne, R.H., 1987. Standardization of standard buffers by visible spectrometry. Anal. Chem. 59 (10), 1479–1481.
Clayton, T.D., Byrne, R.H., 1993. Spectrophotometric seawater pH measurements: total hydrogen ion concentration scale calibration of m-cresol purple and at-sea results. Deep-Sea Res. I Oceanogr. Res. Pap. 40 (10), 2115–2129.
Dickson, A.G., Sabine, C.L., Christian, J.R., 2007. Guide to Best Practices for Ocean CO_2 Measurements. North Pacific Marine Science Organization.
DOE, 1994. Handbook of methods for the analysis of the various parameters of the carbon dioxide system in sea water; version 2. In: Dickson, A.G., Goyet, C. (Eds.), ORNL/CDIAC-74.
Douglas, N.K., Byrne, R.H., 2017. Spectrophotometric pH measurements from river to sea: calibration of mCP for $0 \leq S \leq 40$ and $278.15 \leq T \leq 308.15$ K. Mar. Chem. 197, 64–69.
Easley, R.A., Byrne, R.H., 2012. Spectrophotometric calibration of pH electrodes in seawater using purified m-cresol purple. Environ. Sci. Technol. 46 (9), 5018–5024.
Kadis, R., Leito, I., 2010. Evaluation of the residual liquid junction potential contribution to the uncertainty in pH measurement: a case study on low ionic strength natural waters. Anal. Chim. Acta 664 (2), 129–135.
Liu, X., Patsavas, M.C., Byrne, R.H., 2011. Purification and characterization of meta-cresol purple for spectrophotometric seawater pH measurements. Environ. Sci. Technol. 45 (11), 4862–4868.
Millero, F.J., 1986. The pH of estuarine waters. Limnol. Oceanogr. 31 (4), 839–847.
Millero, F.J., Schreiber, D.R., 1982. Use of the ion pairing model to estimate activity coefficients of the ionic components of natural waters. Am. J. Sci. 282 (9), 1508–1540.
Millero, F.J., Zhang, J.Z., Fiol, S., Sotolongo, S., Roy, R.N., Lee, K., Mane, S., 1993. The use of buffers to measure the pH of seawater. Mar. Chem. 44 (2–4), 143–152.
Müller, J.D., Rehder, G., 2018. Metrology of pH measurements in brackish waters-part 2: experimental characterization of purified m-cresol purple for spectrophotometric pH_T measurements. Front. Mar. Sci. 5, 177.
Nemzer, B.V., Dickson, A.G., 2005. The stability and reproducibility of Tris buffers in synthetic seawater. Mar. Chem. 96 (3–4), 237–242.
Riebesell, U., Fabry, V.J., Hansson, L., Gattuso, J.P., 2011. Guide to Best Practices for Ocean Acidification Research and Data Reporting. Office for Official Publications of the European Communities.
Whitfield, M., Butler, R.A., Covington, A.K., 1985. The determination of pH in estuarine waters. 1. Definition of pH scales and the selection of buffers. Oceanol. Acta 8 (4), 423–432.
Zhang, H., Byrne, R.H., 1996. Spectrophotometric pH measurements of surface seawater at in-situ conditions: absorbance and protonation behavior of thymol blue. Mar. Chem. 52 (1), 17–25.